Research in Astronomy and Astrophysics, 25:025022 (8pp), 2025 February

https://doi.org/10.1088/1674-4527/adb137
CSTR: 32081.14.RAA.adb137

Multi-wavelength Study for Gamma-Ray Nova V1405 Cas

Zi-Wei Ou[1,2], Pak-Hin Thomas Tam[2,3], Hui-Hui Wang[2,3], Song-Peng Pei[4], and Wen-Jun Huang[2,3]
[1] Tsung-Dao Lee Institute, Shanghai Jiao Tong University, Shanghai 201210, China; ouziwei.astro@outlook.com
[2] School of Physics and Astronomy, Sun Yat-Sen University, Zhuhai 519082, China; tanbxuan@sysu.edu.cn
[3] CSST Science Center for the Guangdong-Hongkong-Macau Greater Bay Area, Sun Yat-Sen University, Zhuhai 519082, China
[4] School of Physics and Electrical Engineering, Liupanshui Normal University, Liupanshui 553004, China
Received 2024 November 13; revised 2024 December 31; accepted 2025 January 23; published 2025 February 21

Abstract

Novae are found to have GeV to TeV γ-ray emission, which reveals the shock acceleration from the white dwarfs. Recently, V1405 Cas was reported to radiate suspicious γ-ray by Fermi-LAT with low significance (4.1σ) after the optical maximum. Radio observations reveal that it is one of the five brightest novae surrounded by low-density ionized gas columns. Here we report a continuous search for GeV γ-ray from Fermi-LAT. No γ-ray was found. For V1405 Cas the flux level is lower than other well-studied Fermi novae, and the γ-ray maximum appears at $t_0 + 145$ days. γ-ray of V1405 Cas is used to search potential γ-ray periodicity. No γ-ray periodicity was found during the time of observation. By comparing multi-wavelength data, the γ-ray upper limit to optical flux ratio with a value at around 10^{-4} is obtained to constrain the shock acceleration. Long-term analysis from Swift-XRT gets X-ray spectral in the post-shock phase, which indicates that V1405 Cas became a super-soft source. The best-fit black body temperature at the super soft state is 0.11–0.19 keV.

Key words: gamma-rays: general – (stars:) novae, cataclysmic variables – (stars:) white dwarfs

1. Introduction

A classical nova is one kind of optical transient with a brightness increase by one order in less than a few days (Gallagher & Starrfield 1978). Such transient is an eruption that happens to a white dwarf (WD) which accretes from a main sequence star in a close binary system (Della Valle & Izzo 2020; Chomiuk et al. 2021b). They are different from the so-called "luminous red novae" which are believed to arise from stellar mergers (Cai et al. 2019, 2022, 2022; Pastorello et al. 2019). Classical novae are important objects for studying shock, nucleosynthesis and binary evolution (José et al. 2006). Since WDs undergoing nova eruptions can obtain mass during accretion, novae have been suggested as the progenitors of Type Ia supernovae in degenerate scenarios (Shara et al. 2010; Soraisam & Gilfanov 2015). The shell of WD will be heated by compression and undergo a thermonuclear runaway, which results in the ejection of the accreted mass (Starrfield et al. 2016). Such transient objects observed from radio to γ-ray are identified first by optical observations.

Since the Fermi spacecraft launched in 2008 August, more and more γ-ray novae have been discovered by the Large Area Telescope (LAT) on board Fermi (Ackermann et al. 2014; Franckowiak et al. 2018). Novae can accelerate a fraction of the swept-up particles to high energies by diffusive shock acceleration within the Fermi-LAT detection energy range. Both classical and recurrent novae (e.g., RS Oph) are detected by Fermi-LAT (Cheung et al. 2022). RS Oph is seen even in the TeV range also (H. E. S. S. Collaboration et al. 2017; Acciari et al. 2022). The GeV γ-ray emission from Galactic novae observed by Fermi-LAT reveals that these objects may accelerate relativistic particles by shocks probably (Li et al. 2017). The hadronic origin γ-ray related to proton–proton collisions from novae imply a production of neutrinos (Guépin & Kotera 2017; Fang et al. 2020). For symbiotic novae (e.g., V407 Cyg, RS Oph), this emission is thought to have occurred when this high-velocity material shocked the dense stellar wind from their red giant companion.

The ratio of γ-ray and optical luminosity is suspected to be a key to constraining the lower limit on the fraction of the shock power that accelerates relativistic particles (Metzger et al. 2015). Therefore, simultaneous γ-ray and optical observations would be necessary for Galactic novae. The typical γ-ray novae are transient sources detected over a 2–3 week duration (Ackermann et al. 2014). By assuming all novae are γ-ray emitters, classical novae with $m_R \leqslant 12$ and within $\approx$8 kpc are likely to be discovered in γ-ray using Fermi-LAT (Morris et al. 2017).

Shock acceleration from a nova not only emits γ-ray but also radiates X-rays. The internal shocks from novae have velocities around 1000 km s^{-1} and heat the post-shock gas to temperatures above 10^7 K, which can produce X-ray emission (Steinberg & Metzger 2020). Most γ-ray novae show X-ray evidence of hot shock plasma, but not until the γ-ray has faded below detectability (Gordon et al. 2021). Same as classical novae, the recurrent nova RS Oph was reported to produce X-ray emission originating from shocked ejecta before the X-ray super soft source (SSS) emerged (Orio et al. 2022a).

X-ray emission from classical novae during their γ-ray period could be absorbed by dense ejecta (Metzger et al. 2014).

V1405 Cas (PNV J23244760+6111140) was discovered on 2021 March 18 at 10:10 UT (Wischnewski 2022). Surprisingly, a series of optical flares were found with the brightest one reaching $V = 5.1$ around 2021 May 10. Suspected γ-ray emission has been found after 2021 May 10 with low detection significance, making it as one of the promising γ-ray novae (Buson et al. 2021; Gong & Li 2021). However, the time difference between potential γ-ray and optical is unclear. By using 4 days time bins, it was detected with 4.1σ significance in data from 2021 May 20 15:01:17 to 2021 May 24 15:01:17 UTC with a flux ($E > 100$ MeV) of $(1.4 \pm 0.8) \times 10^{-7}$ photons cm^{-2} s^{-1}. Therefore, it is worthwhile to investigate γ-ray emission for the long term. Accordingly, one can check whether V1405 Cas has a γ-ray emission occurring at a late epoch compared to the other novae. Furthermore, no matter if for significant flux or upper limit, the shock acceleration of a nova may be constrained. In this paper, we investigate γ-ray and X-ray emissions resulting from the shock of V1405 Cas. The paper is organized as follows. Section 2 gives data selection and analysis methods. Section 3 shows the results from γ-ray and X-ray data analysis. Section 4 discusses particle acceleration, white dwarf spinning and the super soft X-ray state. Section 5 summarizes our conclusions.

2. Observations and Analysis

2.1. AAVSO

The optical light curve of V1405 Cas has been collected from the American Association of Variable Star Observers (AAVSO)[5](Percy & Mattei 1993). Coordinates of AAVSO observations for V1405 Cas give: R.A. $= 23^{h}24^{m}48^{s}$, decl. $= 61°11'15''$ (Wischnewski 2022). The optical maxima appears at MJD = 59344.297. Several optical bands are included in the data of the AAVSO database. To put it simply, we use the V band (Johnson V filter, Effective Wavelength = 5448 Å) to generate a light curve (see Figure 1 panel (a)). A galactic reddening of $E(B-V) = 0.32$ mag ($A_V = 1.03$ mag with $R_V = 3.1$) was assumed (Schlafly & Finkbeiner 2011). $(B-V)_0$ of the earliest time (MJD 59293) and the peak time show 0.20 mag and 0.26 mag respectively, corresponding to color temperatures T_c of 7790 K and 7300 K (Kitchin 2013). There is one significant peak in Episode I and several peaks in Episodes II and III the (definition of the three episodes can be seen in Section 2.2).

The magnitude starts from 8.822 at the beginning and rises to 5.082 at MJD of 59344.3, which is the first peak and the maximum of the whole time span. Then the magnitude goes through fluctuation and rises to 5.91 as the second peak, which is located in Episode II. After that, the magnitude continued to go through several periods of slight fluctuation and then decline.

[5] http://www.aavso.org

2.2. Fermi-LAT Observations

Fermi-LAT photon data with energy ranging from 300 MeV to 100 GeV within a 15° search radius are used in this analysis. Coordinates of Fermi-LAT observations for V1405 Cas are: R.A. $= 351.^{\circ}199$, decl. $= 61.^{\circ}1874$ after running `gtfindsrc`. Events with a zenith angle greater than 90° were excluded. The Instrument Response Functions (IRFs) used in this analysis is P8R3_SOURCE_V3. The binned maximum-likelihood analysis (`gtlike`) was performed based on the 4FGL catalog (gll_psc_v27.fit). The Galactic emission gll_iem_v07 and isotropic diffuse emission iso_P8R3_SOURCE_V3_v1 are adopted. For sources within 5° from V1405 Cas the normalization parameters are freed. The spectrum of V1405 Cas is assumed to be a power law (PL):

$$\frac{dN}{dE} = N_0\left(\frac{E}{E_0}\right)^{\Gamma} \tag{1}$$

where N_0 is prefactor in units of cm^{-2} s^{-1} MeV^{-1}, Γ is the power index, E_0 is energy scale in units of MeV.

To improve our starting model before analyzing the nova eruption, we fit a 1 yr data set spanning from 2020 March 18 to 2021 February 18, which ends 30 days before t_0. There is no significant detection at the position of V1405 Cas with a 95% confidence flux upper limit, $\leqslant 3.24 \times 10^{-9}$ ph cm^{-2} s^{-1}. In comparison, γ-ray emission upper limits after t_0 are around 10^{-8} ph cm^{-2} s^{-1}, which will be shown in the next section.

Upper limits at the 90% confidence level (CL) are shown when the test statistic (TS) value is smaller than 4. The Fermi-LAT light curve with 3 days bin from 2021 March 11 is shown. In addition, for comparison with the long-term X-ray observation, a 30 days bin analysis with PL is also performed.

At the same time, we assume an exponential cutoff power law (PLSuperExpCutoff) for Fermi-LAT data to generate a light curve:

$$\frac{dN}{dE} = N_0\left(\frac{E}{E_0}\right)^{\Gamma} \exp\left(-\left(\frac{E}{E_c}\right)^{b}\right) \tag{2}$$

where N_0 is prefactor in units of cm^{-2} s^{-1} MeV^{-1}, Γ is power index, E_0 is energy scale in units of MeV, E_c is cutoff energy in units of MeV, b is the second power index.

2.3. Swift-XRT Observations

The Neil Gehrels Swift Observatory is a rapid-response satellite. The X-ray Telescope (XRT) on board is a focusing telescope which detects an energy range between 0.2 and 10 keV. We selected Swift-XRT observations of exposure time

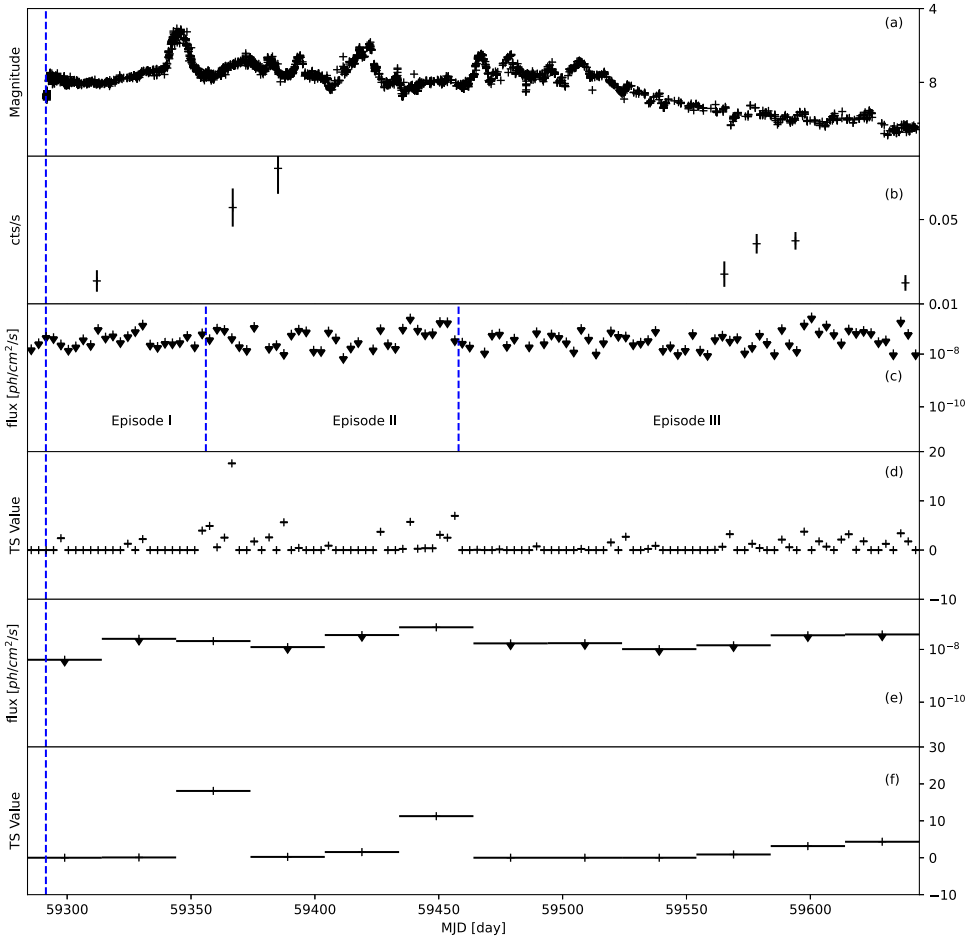

Figure 1. From top to bottom: (a) AAVSO *V* band light curve; (b) Swift-XRT light curve; (c) Fermi-LAT 3 days bin upper limits (PL) with 90% CL; (d) Fermi-LAT 3 days TS value (PL); (e) Fermi-LAT 30 days bin upper limits (PL) with 90% CL; (f) Fermi-LAT 30 days TS value (PL). The blue dashed lines divide the time into different episodes. The red crosses indicate data points with TS values larger than 4.

longer than 1 ks to check the evolution of the spectrum. An absorbed PL model was chosen to fit each observed spectrum based on web-form on the building.

The XRT cleaned event-lists were generated by the pipeline tool `xrtpipeline`. The source image, spectrum and light curve were extracted by `xselect`. Ancillary Response Files (ARFs) were created by using `xrtmkarf`.

According to the Fermi-LAT light curve, we divide Swift-XRT observations into three episodes:

1. *Episode I*. Before MJD 59356, no γ-ray is detected by Fermi-LAT. The optical light curve rises to the maximum (the first peak).
2. *Episode II*. From MJD 59356 to 59458, suspected γ-ray was begun to be detected by Fermi-LAT. The optical emissions arrive the second peak.
3. *Episode III*. After MJD 59458: the γ-ray disappears.

We combine the observations using `xselect`. For Episode I and Episode II, we cannot conduct spectrum due to the low count rate. We only analyze Episode III.

3. Results

3.1. Fermi-LAT Light Curve and Spectrum

From Figure 1, we can see that TS $\geqslant 4$ γ-ray appears around two weeks after the optical maximum. Since we used 3 days bins, we did not get exactly the same results as Buson et al. (2021). t_0 is defined as the discovery date (2021 March 18 10:10:00). For the PL model at time period of $t_0 + 65$ days to $t_0 + 68$ days and $t_0 + 74$ days to $t_0 + 77$ days, we get γ-ray emission. We use the period from $t_0 + 65$ days to $t_0 + 77$ days to make a similar analysis (Figure 2), which gets a photon index of 1.94 and a TS value of 26.9. A binned likelihood was performed based on `gtlike`. The corresponding best-fit

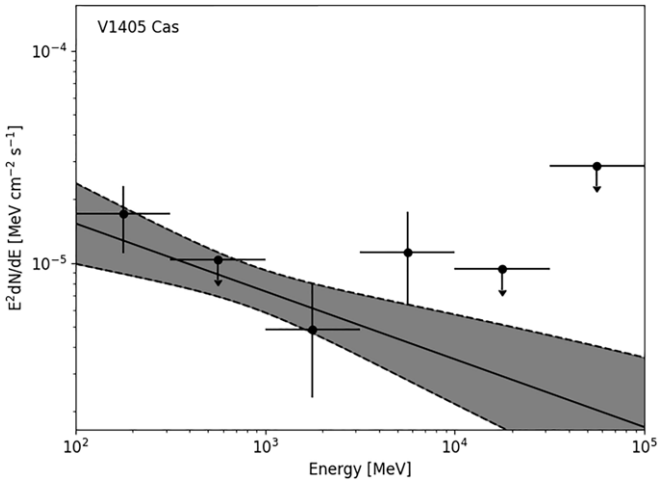

Figure 2. SED of t_0+65 t_0+77 with fixed Γ to −2.3. The dashed lines and gray region indicate the 1σ error of the model. The 95% CL upper limits are also given.

parameters are shown in Table 1. Considering V1405 Cas as a point source, PL and PLSuperExpCutoff are compared. For the PLSuperExpCutoff model, considering $E_c = 3000$ MeV, the significance is slightly higher than that for $E_c = 3000$ MeV. Since the number of free parameters is different, it is hard to draw a conclusion about the best-fitting model.

To investigate shock acceleration, we collect 3 days bin γ-ray data in Figure 1 to calculate the optical and γ-ray flux ratio. The optical flux is calculated by averaging 3 days V band magnitude following $m/M = -2.5\log_{10}(f/F)$, where m and f are magnitude and brightness while M and F are absolute magnitude and absolute brightness. We average the optical flux error bar in each 3 days bin in order to match the γ-ray upper limit and generate a ratio error bar. The corresponding results are shown in Figure 3. The occasional flux ratio is smaller than the ASASSN-16ma value concluded by Li et al. (2017), the RS Oph value revealed by Cheung et al. (2022) and other novae mentioned in Figure 9 of Chomiuk et al. (2021b). This indicates that the internal shock is weaker than that in ASASSN-16ma.

In Figure 4, we compare light curves of well-studied Fermi novae with V1405 Cas.[6] The flux upper limit of V1405 Cas is lower than all the other Fermi novae. The $t = 0$ is defined as the optical maxima of novae. We can see that most Fermi novae have γ-ray maxima in one day to one month after the optical maxima.

3.2. Gamma-Ray Periodicity

Inspired by Li (2022), we search potential GeV γ-ray periodicity of V1405 Cas. An aperture radius of 0.°5 was adopted for pulsation searching. We selected the Fermi-LAT data at the time between t_0 + 65 days and t_0 + 77 days. The arrival time was corrected by `gtbary`. This tool performs a barycentering time correction to an event file using spacecraft orbit files of Fermi-LAT. The selected events are analyzed by using `efsearch` task in the `HEASoft` package (version 6.31.1). `efsearch` is used to search for periodicity in a time series by folding the data over a range of periods. This search is motivated by the 544.84 s γ-ray pulsation detected in nova ASASSN-16ma (Li 2022). After performing a test run from 10 s to 800 s in a resolution of 0.1 s, we did not get any detection. In addition, the Z-test is used to search periodicity also (Kerr 2011). TS for each photon is weighted by its probability using the instrument response function. No periodicity is found.

3.3. X-Ray Spectral Analysis

For investigating the SSS phase, we consider an absorbed blackbody model for Swift-XRT observations in Episode III using an online build Swift-XRT product.[7] Considering the SSS phase, the pile-up characteristics will differ from normal sources. This occurs when several photons hit the detector at the same place between different readouts. As a result, they are counted as one and their energies are summed. Both flux measurements and spectral characteristics would be affected by pipe-up. Selecting this method will cause only grade 0 (single pixel) events to be selected and a lower count-rate threshold to be used when correcting for pile-up. The corresponding best-fit parameters are shown in Table 2, respectively. The information on the Swift observations can be seen in Table 3. The column density of the $N_{\rm H}$ is $\sim 10^{21}$ cm^{-2}. The blackbody temperature kT distributes between 0.1 and 0.2 keV, which indicates that V1405 Cas became an SSS at the post-outburst state.

4. Discussion

4.1. Particle Acceleration and Shock

Figure 1 shows the discrete γ-ray upper limit concurrent with optical emissions (Episode II), which suggests that both are results of shock acceleration from the nova explosion. GeV γ-ray is thought to be the by-product of relativistic particles accelerated by shocks in the nova ejecta (Figueira et al. 2018; Chomiuk et al. 2021b; Acciari et al. 2022). Theoretically, the γ-ray produced by novae is luminous, weighing in at ∼0.1%–1% of the bolometric luminosity predicts that these events could generate photon energies up to 10 TeV, depending on details of the shocks (Metzger et al. 2015). This is verified by simultaneous γ-ray and optical observations of Galactic nova ASASSN-16ma (Li et al. 2017).

[6] https://asd.gsfc.nasa.gov/Koji.Mukai/novae/latnovae.html

[7] https://www.swift.ac.uk/user_objects/

Table 1
Best-fit Parameters Obtained by the Analysis of V1405 Cas Observation with Fermi-LAT from t_0+65 days to t_0+77 days

Spectral Model	Flux (ph cm^{-2} s^{-1})	Γ	E_c (MeV)	b	TS
PL	$1.69 \times 10^{-8} \pm 7.88 \times 10^{-9}$	-1.89 ± 0.29	⋯	⋯	22.726
	$2.50 \times 10^{-8} \pm 4.32 \times 10^{-9}$	−2.3 (fixed)	⋯	⋯	22.293
PLSuperExpCutoff	$9.19 \times 10^{-9} \pm 3.16 \times 10^{-9}$	$-1.14 \times 10^{-5} \pm 0.62 \times 10^{-5}$	2000 (fixed)	1	26.503
	$9.92 \times 10^{-9} \pm 3.72 \times 10^{-9}$	-0.44 ± 0.37	3000 (fixed)	1	28.7199

Note. Columns give (1) spectral model (2) flux, (3) power index, (4) cutoff energy, (5) second power index, and (6) TS value.

According to Figure 1, the X-ray maximum is 20 days after the detection of the most significant γ-ray emission. Thermal X-rays can be produced in the internal shocks that radiate the observed γ-ray emission. One would expect to observe much brighter thermal X-ray emission at around 10 to 1000 times more luminous than the γ-ray flux. In our case, simultaneous X-ray and γ-ray observations of V1405 Cas at Episode II could constrain the radiative efficiency and the particle acceleration efficiency of the internal shocks. The presence of X-ray shock signatures sometimes coincident with the γ-ray results from the small columns of neutral gas around this nova.

Hybrid acceleration of leptons and hadrons in the nova shock has been considered in some research (Martin & Dubus 2013). In that model, the magnetic field is obtained assuming an equipartition with the thermal energy density upstream of the shock. It results in the maximum energy of protons estimated to be ∼300 GeV. The GeV γ-ray emission is then mostly expected from leptonic processes, namely the IC scattering of the nova light by the electrons accelerated in the shock. However, hadronic and/or leptonic-hadronic models are favored to explain the gamma-ray emission of novae taking into account the energy loss of electrons via synchrotron emission (Chomiuk et al. 2021b; De Sarkaret al. 2021b). The narrow energy range at SED of V1405 Cas makes it hard to constrain hadronic or leptonic origins.

4.2. Whether V1405 Cas Contains a Spinning White Dwarf?

Unsurprisingly, a spinning white dwarf can produce gamma-rays like a spinning neutron star (Takata et al. 2017; Munari et al. 2022; Orio et al. 2022b), for example, the misalignment between axes of the WD spin, magnetic dipole, and orbital revolution produce γ-ray pulsations. The nova progenitor is likely a fast-spinning magnetic WD, mostly an intermediate polar Orio et al. (1992). Strong bipolar nova winds from the magnetic poles of the WD regularly interact with the matter deposited into the orbital plane by the early and slow ejection (Orio et al. 2022a). Therefore, it is suitable to ask whether V1405 Cas is spinning, which accelerates electrons to produce GeV γ-ray.

Previously, pulsations of nova are discovered on X-ray from V1674 Her and γ-ray from ASASSN-16ma (Drake et al. 2021; Li 2022). However, no γ-ray pulsation was detected from V1405 Cas due to low photon counts. Nevertheless, this cannot exclude V1405 Cas as a spinning WD (Section 3.2). More observations are needed to classify whether the WD V1405 Cas is spinning or not.

4.3. Super Soft Source

An SSS is one kind of X-ray transient that is always believed to appear in post-outburst novae, in which hydrogen burning continues near the surface after the bulk of accreted envelope mass has been ejected (Orio et al. 2022b). From Table 2 we can see that V1405 Cas is an SSS characterized by soft X-ray emissions. Such a super soft phase appears after shock emergence. The spectra in some novae in the super soft X-ray phase may have redshift velocity of the emission lines and blueshift velocity of the absorption lines (Pei et al. 2021). The flux variation in some emission lines may result from the surrounding cool inhomogeneous material or temporary ionization.

Radio observations from VLA and uGMRT reveal that V1405 Cas are among the five brightest novae ever observed in the radio band, and the expansion velocity is 1200 km s^{-1} (Chomiuk et al. 2021a; Nayana et al. 2022). Such high velocity can heat the gas, which produces X-ray emission at the post-shock phase. The appearance of radio emissions when the γ-ray was detected by Fermi-LAT results from the low-density columns of ionized gas. As expected, V1405 Cas has begun to display Fe II absorption features and then an SSS (Page et al. 2021; Shore et al. 2021). Thus, it becomes an excellent target to study the SSS after shock acceleration. This Fe II absorption points to the nova formation in a large circumbinary envelope of gas (Williams 2012; Aydi et al. 2024). The gas may have an origin of the secondary star.

The typical range of effective temperature $T_{\rm eff}$ in the SSS varies from $\sim 1.2 \times 10^5$ K to about 10^6 K (Suleimanov et al. 2003). The

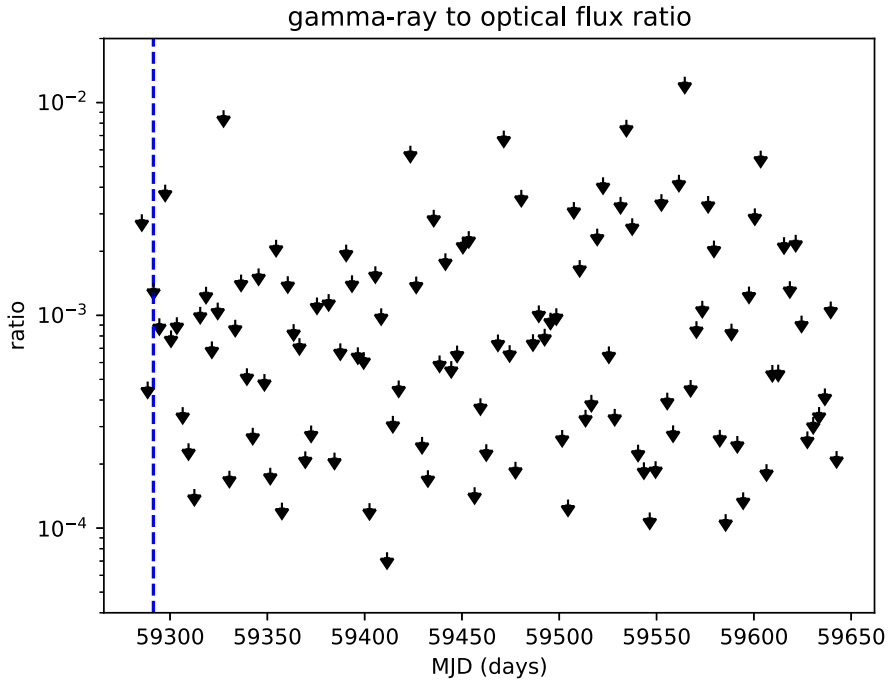

Figure 3. The ratio of γ-ray upper limit to optical flux in Episode II. The blue dashed line gives the optical eruption time.

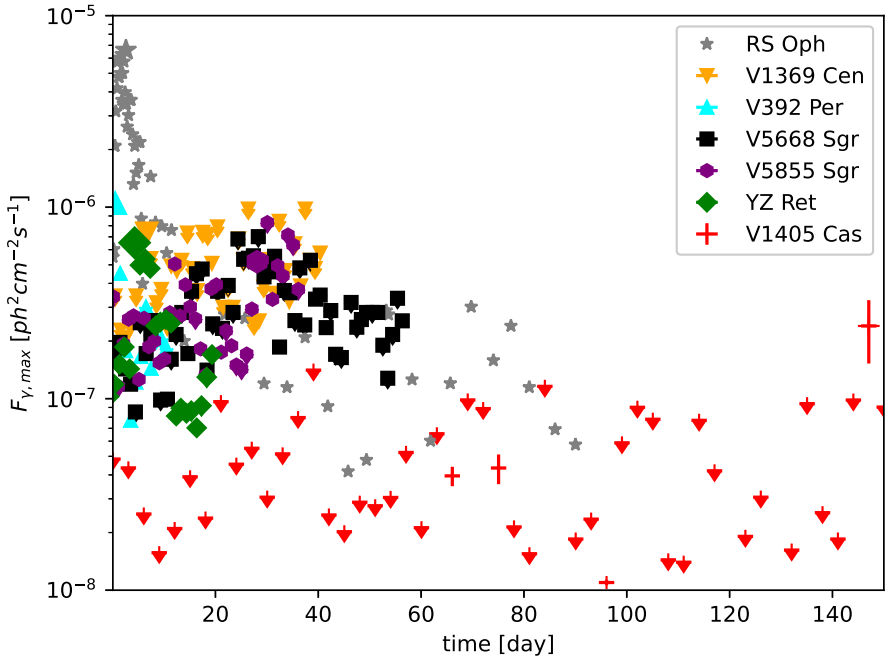

Figure 4. Well-studied Fermi-LAT novae with known light curves. Reference: RS Oph (Cheung et al. 2022); V1369 Cen (Cheung et al. 2016); V392 Per (Albert et al. 2022); V5668 Sgr (Cheung et al. 2016); V5855 Sgr (Nelson et al. 2019); YZ Ret (Sokolovsky et al. 2022); V1405 Cas (this work). For the *X*-axis, Time [day] = 0 corresponding to the optical eruption time for each nova. All the light curves are generated using 1 day bin, except to RS Oph and V1405 Cas. The light curve of RS Oph shows various time bin according to the orbit-timescale of 60 minutes, 6 hr, 1 day and 4 days. The light curve of V1405 Cas is binned into 3 days as mentioned previously.

Table 2
Best-fit Parameters of Blackbody Model (0.3–6.7 keV)

ObsID	$N_{\rm H}$ (10^{21} cm^{-2})	kT (keV)	$F_{\rm un}$ (erg cm^{-2} s^{-1})	η (erg cm^{-2} ct^{-1})	W/dof
00014197018	4^{+6}_{-3}	$0.13^{+0.06}_{-0.05}$	$3.2^{+20.3}_{-2.4} \times 10^{-12}$	1.83×10^{-11}	33.57/27
00014197020	$1.4^{+2.4}_{-1.4}$	$0.19^{+0.06}_{-0.05}$	$1.26^{+2.09}_{-0.55} \times 10^{-12}$	1.81×10^{-11}	45.67/51
00014197024	$6.1^{+10.4}_{-6.1}$	$0.11^{+0.16}_{-0.05}$	$7^{+62}_{-7} \times 10^{-12}$	1.95×10^{-11}	16.3/26

Note. Columns give (1) observation ID, (2) column density of the neutral Hydrogen, (3) blackbody temperature, (4) unabsorbed Flux, (5) flux to count-rate ratio, and (6) fit W/degrees of freedom.

Table 3
Basic Information of Swift-XRT Observations

ObsID	Exposure (ks)	Date	t_0+ (days)
00014197001	0.28	2021-03-24T01:29:03	5.7
00014197002	1.64	2021-03-28T18:10:40	10.4
00014197003	1.85	2021-03-31T08:19:03	12.9
00014197004	1.57	2021-04-03T09:32:43	16.0
00014197005	0.44	2021-04-06T18:47:32	19.4
00014197006	1.83	2021-04-07T20:28:09	20.5
00014197007	1.37	2021-04-09T04:14:48	21.8
00014197008	1.42	2021-04-23T06:25:45	35.9
00014197009	1.90	2021-04-30T02:12:33	42.7
00014197010	1.80	2021-05-07T00:03:15	49.6
00014197011	1.08	2021-05-14T16:44:50	57.3
00014197012	0.92	2021-05-31T00:23:35	73.6
00014197013	0.84	2021-06-15T07:23:29	88.9
00014197014	1.58	2021-06-30T11:45:17	104.1
00014197015	0.73	2021-07-15T11:56:53	119.1
00014197016	0.78	2021-07-30T04:06:01	133.8
00014197017	1.04	2021-12-14T01:51:28	270.7
00014197018	1.89	2021-12-15T00:03:15	271.6
00014197019	1.29	2021-12-29T14:44:10	286.2
00014197020	2.36	2022-01-14T09:35:17	302.0
00014197024	2.34	2022-02-23T03:46:02	341.8

Note. Columns give (1) observation ID, (2) exposure time, (3) observation start date, (4) time since the optical eruption.

low emission during the SSS phase can be explained by absorption from neutral and/or ionized medium (Ness et al. 2023). V1405 Cas has a typical temperature of SSS. For example, RS Oph has a blackbody temperature in the 35–40 eV (≈405,000–470,000 K) range (Orio et al. 2023). V2491 Cyg has a temperature of 90 ± 1 eV (10^6 K) and an X-ray luminosity of 178 × 10^{36} erg s^{-1} (Ness et al. 2022). The temperature is proportional to the shock velocity. Typical soft X-ray photons are absorbed in the ISM with values of $N_{\rm H}$ in several 10^{21} cm^{-2}. As X-rays suffer photoelectric absorption, $N_{\rm H}$ reflects these effects, which is also the case for novae (Nelson et al. 2019). Possibly, the X-ray and γ-ray originated from different regions (Metzger et al. 2015). The $N_{\rm H}$ values of V1405 Cas are around 1.0×10^{21} cm^{-2} to 1.6×10^{22} cm^{-2}. However, resulting from the low quality of X-ray data, we cannot derive the evolution of $N_{\rm H}$.

5. Conclusion

We summarize our conclusion as follows. (1) Typical γ-ray novae show significant γ-ray after the optical maxima in weeks to months. Our result shows that no significant GeV γ-ray emissions of nova V1405 Cas were detected before and after the optical maxima. (2) Typical γ-ray novae have γ-ray maxima at hours to weeks after optical maxima. Our result reveals that the γ-ray upper limit of nova V1405 Cas shows a maximum at t_0 + 145 days. (3) Some classical novae were found to have periodicity in γ-ray emission. We search γ-ray periodicity in V1405 Cas using two methods: `efsearch` and Z-test. Owing to low GeV photon counts, no γ-ray periodicity is found from Fermi-LAT. (4) X-ray emission of novae arrives at a soft phase. Our work introduces an adsorb blackbody model to investigate the potential SSS phase. We show that V1405 Cas turned to a super soft state after γ-ray emissions disappeared according to the best-fit temperature values. (5) γ-ray to optical ratio is a key for shock acceleration, our result shows a ratio around 10^{-4}–10^{-2} which approaches bright γ-ray novae (e.g., ASASSN-16ma, RS Oph).

Although some novae have low significance and weak signals in γ-ray, it is still valuable to observe such objects. With higher sensitivity, the future Very Large Area Gamma-Ray Space Telescope (VLAST) may improve that (Fan et al. 2022). X-ray telescopes, such as Einstein Probe (EP) and Space-based multi-band astronomical Variable Objects Monitor (SVOM), would also help us to unveil SSS nature for more novae.

Acknowledgments

The authors thank Kwan-Lok Li for many useful discussions. Scientific results from data presented in this publication are obtained from AAVSO and HEASARC. Z.W.O. is supported by the National Natural Science Foundation of China (NSFC, grant No. 12393853). P.H.T., H.H.W. and W.J.H. are supported by the NSFC under grant 12273122. H.H.W. is supported by the Scientific Research Foundation of

Hunan Provincial Education Department (21C0343). S.P.P. is supported by the Science Research Project of the University (Youth Project) of the Department of Education of Guizhou Province (QJJ[2022]348) and the Science and Technology Foundation of Guizhou Province (QKHJC-ZK[2023]442).

ORCID iDs

Zi-Wei Ou https://orcid.org/0000-0002-3632-474X
Song-Peng Pei https://orcid.org/0000-0002-0851-8045

References

Acciari, V. A., Ansoldi, S., Antonelli, L. A., et al. 2022, NatAs, 6, 689
Ackermann, M., Ajello, M., Albert, A., et al. 2014, Sci, 345, 554
Albert, A., Alfaro, R., Alvarez, C., et al. 2022, ApJ, 940, 141
Aydi, E., Chomiuk, L., Strader, J., et al. 2024, MNRAS, 527, 9303
Buson, S., Cheung, C. C., & Jean, P. 2021, ATel, 14658, 1
Cai, Y., Reguitti, A., Valerin, G., & Wang, X. 2022, Univ, 8, 493
Cai, Y. Z., Pastorello, A., Fraser, M., et al. 2019, A&A, 632, L6
Cai, Y. Z., Pastorello, A., Fraser, M., et al. 2022, A&A, 667, A4
Cheung, C. C., Jean, P., Shore, S. N., et al. 2016, ApJ, 826, 142
Cheung, C. C., Johnson, T. J., Jean, P., et al. 2022, ApJ, 935, 44
Chomiuk, L., Linford, J. D., Aydi, E., et al. 2021a, ApJS, 257, 49
Chomiuk, L., Metzger, B. D., & Shen, K. J. 2021b, ARA&A, 59, 391
De Sarkar, A., Nayana, A. J., Roy, N., Razzaque, S., & Anupama, G. C. 2023, ApJ, 951, 62
Della Valle, M., & Izzo, L. 2020, A&ARv, 28, 3
Drake, J. J., Ness, J.-U., Page, K. L., et al. 2021, ApJL, 922, L42
Fan, Y. Z., Chang, J., Guo, J. H., et al. 2022, AcASn, 63, 27
Fang, K., Metzger, B. D., Vurm, I., Aydi, E., & Chomiuk, L. 2020, ApJ, 904, 4
Figueira, J., José, J., Garcìa-Berro, E., et al. 2018, A&A, 613, A8
Franckowiak, A., Jean, P., Wood, M., Cheung, C. C., & Buson, S. 2018, A&A, 609, A120
Gallagher, J. S., & Starrfield, S. 1978, ARA&A, 16, 171
Gong, Y.-H., & Li, K.-L. 2021, ATel, 14620, 1
Gordon, A. C., Aydi, E., Page, K. L., et al. 2021, ApJ, 910, 134
Guépin, C., & Kotera, K. 2017, A&A, 603, A76
H. E. S. S. Collaboration, Aharonian, F., Ait Benkhali, F., et al. 2022, Sci, 376, 77
José, J., Hernanz, M., & Iliadis, C. 2006, NuPhA, 777, 550
Kerr, M. 2011, ApJ, 732, 38
Kitchin, C. R. 2013, Astrophysical Techniques (Boca Raton, FL: CRC Press)
Li, K.-L. 2022, ApJL, 924, L17
Li, K.-L., Metzger, B. D., Chomiuk, L., et al. 2017, NatAs, 1, 697
Martin, P., & Dubus, G. 2013, A&A, 551, A37
Metzger, B. D., Finzell, T., Vurm, I., et al. 2015, MNRAS, 450, 2739
Metzger, B. D., Hascoët, R., Vurm, I., et al. 2014, MNRAS, 442, 713
Morris, P. J., Cotter, G., Brown, A. M., & Chadwick, P. M. 2017, MNRAS, 465, 1218
Munari, U., Giroletti, M., Marcote, B., et al. 2022, A&A, 666, L6
Nayana, A. J., Anupama, G. C., Banerjee, D., et al. 2022, ATel, 15383, 1
Nelson, T., Mukai, K., Li, K.-L., et al. 2019, ApJ, 872, 86
Ness, J. U., Beardmore, A. P., Bezak, P., et al. 2022, A&A, 658, A169
Ness, J. U., Beardmore, A. P., Bode, M. F., et al. 2023, A&A, 670, A131
Orio, M., Behar, E., Luna, G. J. M., et al. 2022b, ApJ, 938, 34
Orio, M., Gendreau, K., Giese, M., et al. 2022a, ApJ, 932, 45
Orio, M., Gendreau, K., Giese, M., et al. 2023, ApJ, 955, 37
Orio, M., Trussoni, E., & Oegelman, H. 1992, A&A, 257, 548
Page, K. L., Starrfield, S., Munari, U., Woodward, C. E., & Wagner, R. M. 2021, ATel, 15111, 1
Pastorello, A., Mason, E., Taubenberger, S., et al. 2019, A&A, 630, A75
Pei, S., Orio, M., Ness, J.-U., & Ospina, N. 2021, MNRAS, 507, 2073
Percy, J. R., & Mattei, J. A. 1993, Ap&SS, 210, 137
Schlafly, E. F., & Finkbeiner, D. P. 2011, ApJ, 737, 103
Shara, M. M., Yaron, O., Prialnik, D., & Kovetz, A. 2010, ApJL, 712, L143
Shore, S. N., Buil, C., Dubovsky, P., et al. 2021, ATel, 14577, 1
Sokolovsky, K. V., Li, K.-L., Lopes de Oliveira, R., et al. 2022, MNRAS, 514, 2239
Soraisam, M. D., & Gilfanov, M. 2015, A&A, 583, A140
Starrfield, S., Iliadis, C., & Hix, W. R. 2016, PASP, 128, 051001
Steinberg, E., & Metzger, B. D. 2020, MNRAS, 491, 4232
Suleimanov, V., Meyer, F., & Meyer-Hofmeister, E. 2003, A&A, 401, 1009
Takata, J., Yang, H., & Cheng, K. S. 2017, ApJ, 851, 143
Williams, R. 2012, AJ, 144, 98
Wischnewski, E. 2022, BAVMS, 11, 6